Electronic and geometric structure of Si(111)-5×2-Au

H. S. Yoon, J. E. Lee, S. J. Park, and I.-W. Lyo*

Institute of Physics and Applied Physics, Yonsei University, Seoul 120-749, Korea

M.-H. Kang

Department of Physics, Pohang University of Science and Technology, Hyoja-dong, Pohang 790-784, Korea

Si(111)-5×2-Au is investigated in detail using scanning tunneling microscopy and spectroscopy at 78 K. It is shown that topographic features in STM images are strongly dependent on bias voltages, including a new atomic feature, V unit. Detailed investigations of local distributions of electronic states by scanning tunneling microscopy, point spectroscopy, and current imaging tunneling spectroscopy suggest extensive charge transfers between intra- and interlocal unit cells. Comparisons of experimental and theoretical structural models proposed up to date are made and it is found that none of models truly reproduces all the features observed so far. Our findings suggest that further investigation is required.

I. INTRODUCTION

A low-dimensional system has been extensively studied for a number of years due to its novel electronic properties and possible device applicability. Particularly, metal on semiconductor systems have drawn a lot of interest because they are found to be easily fabricated to low-dimensional, especially one-dimensional, structures with tailored electronic properties.

Recently, Au/Si(111) systems have become fascinating, due to the report of an unusual ground state. A one-dimensional metallic band observed on a highly stepped Si(111) has been proposed to have spin-charge separation, an evidence of the Luttinger liquid.[1]

Si(111)-5×2-Au, which is one of various phases[2,3] found when a submonolayer of Au is deposited on clean Si(111) surface, is a self-organized one-dimensional system with the two rows of weakly dimerized substitutional Au chains along $[1\bar{1}0]$.[4–6] Although these rows are not imaged, scanning tunneling microscopy (STM) studies revealed a complex surface structure[7–10] and a preferential growth from step edges.[11–15] Angle-resolved photoemission studies found that the system is metallic,[16] however, more recently it was suggested to be nonmetallic with up to a 0.3 eV gap,[17–19] although it was commonly agreed that the system is one dimensional electronically as well as optically.[20]

Reflecting interests on the system, a few experimental models[6,9,10,14,15,21] as well as a recent theoretical model[22] have been proposed. Among these models, the identity and location of a feature called a bright protrusion (BP) plays a central role, which always appears on the Si(111)-5×2-Au surface. However, they had been no consensus on the identification of bright protrusions. It had been suggested that bright protrusions are either Au adatoms[7,13–15,23,24] or Si adatoms.[8] But a recent study using STM strongly supports that bright protrusions are Si adatoms,[25] although the rest of the structure remains still unclear. Interestingly these bright protrusions were proposed as a possible atomic scale memory at silicon surface capable of a terabit storage when

atomically manipulated using STM.[26] A recent theoretical investigation[27] showed that two major proposed models[6,15] do not reproduce key features observed by photoemission and STM. Thus the correct structure model for Si(111)-5×2-Au is still lacking.

In this paper, the geometric and electronic structures of Si(111)-5×2-Au are examined in detail using high-resolution STM and scanning tunneling spectroscopy (STS) at low temperature. Our results revealed a topographical transition in STM images depending on bias voltages that have not been observed in prior works. A new atomic feature, V unit, and a local distribution of electronic states are observed by STM, point STS, and current imaging tunneling spectroscopy (CITS). Influences of state D and a Si adatom are found to be critical on both the geometric and electronic structure. In addition, recently proposed structure models of Si(111)-5×2-Au will be discussed based on our STM images.

II. EXPERIMENTAL PROCEDURE

The experiment were carried out with an UHV system consisting of an analysis chamber and a preparation chamber that were used elsewhere.[28] All standard sample preparations including sample cleaning, Au deposition, and a low-energy electron diffraction (LEED) measurement were performed in the preparation chamber. Then samples were transported to the analysis chamber equipped with commercial Omicron LT-STM after sample preparations. At the base pressure less than 2×10^{-10} mbar, the clean Si(111) surface was obtained from a wafer vicinally oriented by 4 deg toward the $[11\bar{2}]$ direction, by 920 K annealing for more than 24 h and several cycles of 1480 K flashing for the duration of 3 s. Au was deposited from a tungsten filament at 940 K at a rate lower than 0.01 ML/s and surface quality and coverage proper to the STM measurement were monitored by LEED. STM measurements were performed at a base pressure below 3×10^{-11} mbar, and liquid nitrogen temperature (78 K). Point
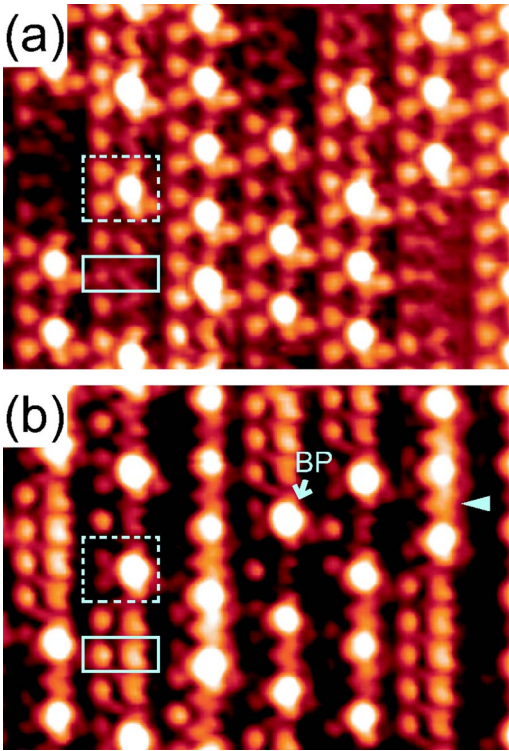
FIG. 1. (Color online) Large-scale typical STM images in a filled state (a), and an empty state (b). Rectangular 5×2 and 5×4 units are depicted by solid lines and dashed lines, respectively. Bright protrusions are imaged as white spots at both filled and empty states. Bias voltages are (a) -0.4 V and (b) $+0.7$ V and the tunneling current is 0.1 nA.

STS measurements were performed for up to 20 s over individual sites to enhance the statistics, during which the drift rate was kept to less than 0.03 nm/min. In CITS, $1-2$ s were used for $I(V)$ measurement at each pixel of an image. All data presented here were acquired at liquid nitrogen temperature. Although STM imaging was performed at room temperature as well, essentially no difference was found between 78 K and room temperature results, besides better resolution and less thermal drift due to enhanced stability at low temperature.

III. TOPOGRAPHIC FEATURES IN STM IMAGES

Figure 1 shows typical STM images of the Si(111)-5$\times$2-Au surface, obtained simultaneously over the same area. A rectangle in solid lines in the images marks a unit cell of 5×2. Baski *et al.* termed two main features in the rectangular unit cell a "round unit" and a "rectangular unit" from their empty state images.[8]

As shown in our better resolved image, Fig. 1(b), however, the so-called rectangular unit clearly does not appear rectangular. Two small tails are apparent on one side. Henceforth they will be called in our work "U units," instead of rectangular units, in order to avoid possible confusions. Furthermore, a feature marked by an arrowhead was labeled as triangular units in previous works, however, in this paper, it will be called a "V unit" in the same vein. The reasons behind this relabeling will be discussed later. V units are found between two bright protrusions separated by only $4a_0$ [a_0 is a Si(111) unit length, 0.387 nm] under the tunneling condition specified in Fig. 1(b). The counterpart in the filled state is signified by a presence of a nodelike feature in the middle. Note also that in the filled state image of Fig. 1(a), U units appear V shaped. However, these U units are not V units because they are found only in the region where two bright protrusions are separated by $6a_0$ or more. In conjunction with a round unit in the same cell, the U unit forms a "Y" feature, as previously described.[9,10]

Bright protrusions are typically located between two neighboring U units, located on the same row running in the $[1\bar{1}0]$ direction. A spacing between bright protrusions is a multiple of $2a_0$ because U units have a $2a_0$ periodicity. However, the spacing, $2a_0$, was seldom found in our data. This is attributed to apparent nearest neighbor repulsion interaction[24,29] between BPs. Consequently, they form short chains spaced by $4a_0$, which is the actual minimum spacing, and terminated by a BP-free segment of $2na_0$, where n is an integer. One bright protrusion and two round features constitute a local 5×4 unit cell (dotted lines in Fig. 1) and the short chains of these units were found to exhibit very interesting features.[30] As mentioned earlier, the identity of bright protrusions had been under question for a long time, and suspected to be Au adatoms.[7,13–15,23,24] However, the recent experiments with additional deposition of Si and Au onto initial Si(111)-5$\times$2-Au surface favored Si adatoms,[25] and our own experiments also produced similar results.

IV. BIAS-DEPENDENT FEATURES IN STM IMAGES

In order to construct an improved Si(111)-5$\times$2-Au structure, it would be informative to first examine the bias dependence of STM images. Our high-resolution STM images with various bias dependence are summarized in Fig. 2. Figure 2(a) is a filled-state image and Figs. 2(b)–2(f) are empty-state images of the same area. The images show each row labeled 1 through 4 include two Si adatoms spaced apart by 4, 8, 6, and 4 a_0's. The first thing to note is that Si adatoms (bright protrusions) are prominent throughout the whole bias voltages. On the other hand, in a filled state [Fig. 2(a)], round units and U units are imaged brightly. At an empty state [Fig. 2(b)] near the Fermi level, two units are imaged similar to the filled state image, but U units now have thicker bridges than in the filled state, resulting in U units that look like rectangular shapes, as mentioned above. Interestingly, a dramatic change occurs in STM images as the bias voltage increases. At +0.65 V, as shown in Fig. 2(c), while round and U units show no change, the interval between the two Si adatoms that belong to a $4a_0$-spaced Si adatom chain turn bright in row 4 and produce a V unit. At +0.75 V, as in Fig. 2(d), 0.1 V higher than that of Fig. 2(c), V units emerge, even in Si adatom-free regions. Notice that U and V units begins to overlap on row 2 as V units emerge, while U units on row 3 has already disappeared. BP-free segments over a two-unit length show the same feature as two-unit length BP-free segments (not shown here).
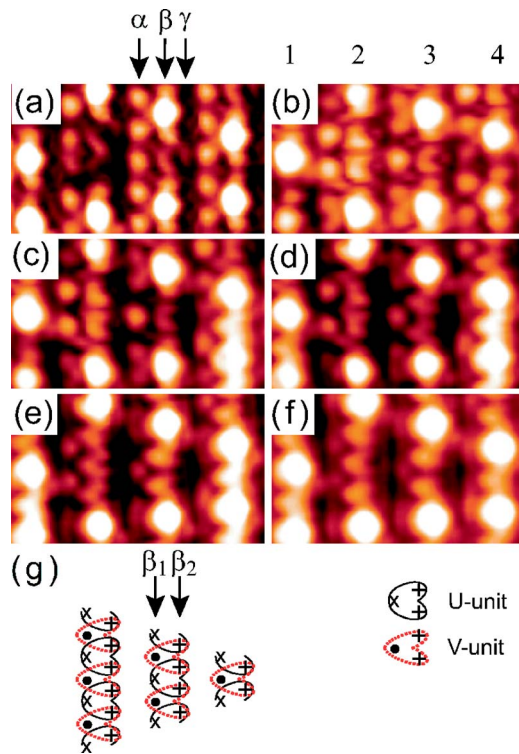
FIG. 2. (Color online) Zoomed STM images with various bias voltages over the same site. Bias voltages are (a) −0.5 V, (b) +0.3 V, (c) +0.65 V, (d) +0.75 V, (e) +0.85 V, and (f) +1.0 V. The tunneling current is set to 0.1 nA. Each row is labeled by numbers 1 through 4. (g) A schematic diagram of topographical features corresponding to rows 2 to 4 between two Si adatoms.

FIG. 3. (Color online) Normalized dI/dV spectra acquired on three different atomic sites α, β, and γ. Five states labeled from A to D are recognized clearly in the spectra. Imaging conditions before measuring spectroscopy are $V_b = -1.5$ V and $I_t = 1.0$ nA. The bias voltage and tunneling current for an inset are +0.7 V and 0.1 nA, respectively.

Drastic changes observed in STM images at higher than +0.7 V have not been reported before. At +0.85 V, as shown in Fig. 2(e), all U units are fully transformed to V units. In addition, round units gradually lose their intensities as the bias voltage is increased before almost disappearing at Fig. 2(e) for round units with Si adatoms in the same local unit cell. Finally at +1.0 V, V units appear triangle shaped because inner areas of V units are equally bright. Note also that above this bias, a pair of lines emerge between rows, as shown in Fig. 2(f). Among pairs of lines, right-hand side lines are from the round units, whereas the origin of left-hand side lines will be discussed in later sections.

It is easy to recognize that U and V units are geometrically out of phase with each other. A schematic diagram is presented in Fig. 2(g) to explain the phase relations, where U and V units are depicted by solid lines and dotted lines, respectively.

Each local unit at Si(111)-5×2-Au surface consists of 3 different $[1\bar{1}0]$ sub-rows, namely, α, β, and γ, which designate a row of round units, a row of U units (V units), and a row of the dark region, respectively. Furthermore, row β, that of U units and V units, appears to have at least two subcomponents of bright features, β_1 and β_2. As shown in Fig. 2(g), row β_1 is composed of crosses and dots, and β_2 of pluses. Then the topographic transition between U and V units may be interpreted as follows. At a low empty bias, pluses, and crosses are responsible for bright features in

STM images, forming U units. As the bias is increased, however, crosses lose their intensity while pluses do not, and dots gain intensity, resulting in V units. Thus, bias-dependent intensities of each subcomponent such as crosses and dots may form the topographical features in STM images.

The alternating occurrence of two different sites in STM images are due to the local distribution of the density of states (DOS), particularly in an empty state. In order to investigate the DOS of Si(111)-5×2-Au, site-specific tunneling spectra, I vs V, were measured, as shown in Fig. 3. A normalized (dI/dV) curve, $(dI/dV)/(I/V)$, may be taken as an approximation of local DOS. Five distinctive surface states were found, and designated A to E. The primed states A' to C' denote segments without Si adatoms. As shown in Fig. 3, BP-free segments are metallic due to the nonzero LDOS at E_F. On the other hand, Si adatom chains that are spaced by $4a_0$ are semiconducting, as represented by site 1 in Fig. 3. A pair of B and C, or B' and C', look like half-filled dangling bonds states or π, π^* states of Si(001)-2×1. Note that spectra over sites 2 and 3 are qualitatively similar to each other, indicating that the LDOS are strongly delocalized, with the exception of state D. State D is exceptionally intense at site 3, because of its strong spatial localization and proximity to row β_1. It is localized at the dot subunit site, as denoted in Fig. 2, along row β_1. On the other hand, state C' has high LDOS and appear relatively stronger at site 2. State E appear widely delocalized over the whole surface.

We find that the apparent topographic shift from U units to V units is strongly correlated with state D. The contribution to a tunneling current comes from LDOS between E_F
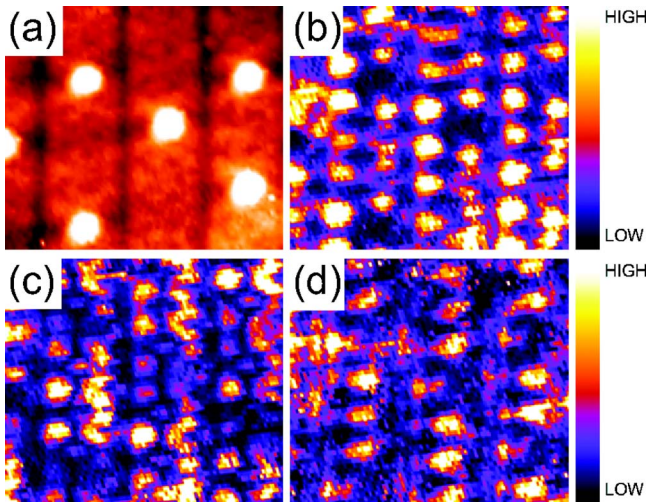
FIG. 4. (Color online) dI/dV maps obtained by CITS. (a) is a topographic image acquired simultaneously with $I(V)$. The bias voltage and tunneling current are −1.5 V and 2.0 nA, respectively. (b), (c), and (d) represent LDOS maps at states B', C', and D, respectively.

FIG. 5. (Color online) Line profiles of a row of round units with or without a Si adatom. Round units beside Si adatoms are imaged less or more brightly in the (a) empty or (b) filled state image, respectively. Bias voltages are (a) +0.3 V and (b) −0.3 V and the tunneling current is 0.1 nA.

and a bias voltage, with the convolution of the transmission factor. Thus, at the bias voltage less than +0.65 V, which corresponds to Figs. 2(a) and 2(b), the contribution to STM images comes only from state C', and U units appear in accordance with the local distribution of state C'. At +0.65 eV, where state D lies, state D now begins to contribute to STM images and new bright feature emerges at dot subunit sites, as shown in Fig. 2(c). Above +0.65 eV, the contribution of state D dominates over state C', leading to V units. Beyond +0.85 eV, only V units stay bright, in addition to ever-bright Si adatoms. Throughout the bias range considered, plus subunits stay persistently bright, while cross subunits disappear above +0.85 eV, as shown in Fig. 2(e). Thus plus and cross subunits represent mutually distinctive chemical states.

CITS technique using scanning tunneling microscopy is useful for investigating the distribution of LDOS at a particular energy.[31] CITS is the measurement of local $I(V)$ data at every pixel of an STM image while maintaining constant tip-sample separation by keeping the tunneling condition fixed. Our CITS results are shown in Fig. 4. The topographic image [Fig. 4(a)], simultaneously acquired with CITS [Figs. 4(b)–4(d)], does not reveal the surface in detail, because its tunneling condition, −1.5 V and 2.0 nA, was set as far away as possible from E_F so as to obtain good tunneling spectra. On the other hand, dI/dV maps from (b) to (d) clearly demonstrate that states B' and C' are found as round and U units, while state D is restricted to dot sites.

In these images, Au rows are not directly imaged by STM. The bands produced by Au $5d$ electrons are not only located from −4.2 to−6.0 eV, well out of the STM window, but also too compact to be imaged.[16] However, highly dispersive Si−Au bonds may be weakly imaged in the empty state. In Fig. 4(d), as in Fig. 2(f), a pair of linear lines emerge. The right-hand side lines line up with the round unit rows, as horizontally aligned figures in Fig. 2 demonstrates. On the
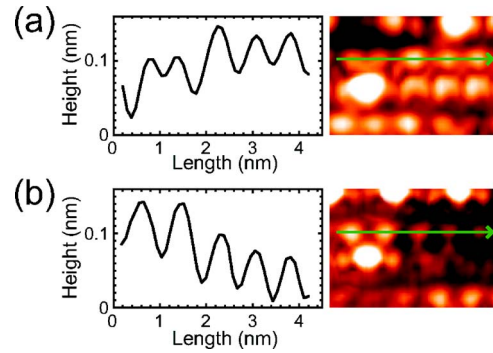
other hand, the left-hand side lines corresponds to previous dark rows γ, and yet both sides of the left-hand side lines are still separated by dark lines.

The presence of Si adatoms induce changes in electronic states of adjacent round units. Figures 5(a) and 5(b) show line profiles of round units (row α) at empty and filled states, respectively. They were acquired simultaneously at the same site through a dual-bias scanning method. Two round units adjacent to a Si adatom appear weak in the empty state, while they appear strong in the filled state. Charge transfer from a dangling bond of a Si adatom to two adjacent round units would increase LDOS of filled state B, while decreasing that of empty state C. This trend is also found strong in the upper spectrum in Fig. 6(a), where states B and C appear weak. The same tendency is also clearly observable in dI/dV images of states B and C, as shown in Figs. 4(b) and 4(c), respectively. A local 5×4 structure is favored over local 5×2 with Si adatoms due to strong nearest-neighbor repulsion.[24,29] This repulsion may be attributed to the significant reduction in the number of round units per Si adatoms in the case of 5×2 with Si adatoms, where each Si adatom has to share a round unit, and thus charge transfer becomes limited.
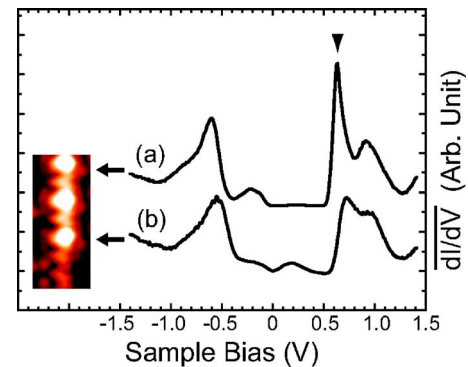
FIG. 6. (Color online) Normalized dI/dV curves (a) inside and (b) outside a local 5×4 chain. The intensity and width of the state D indicated by an arrowhead are stronger and narrower outside the chain than inside the chain. It is also observed that the state B is increased and the state C is decreased inside the chain. Imaging conditions for the inset is $V_B = +0.85$ V and $I_t = 0.1$ nA.
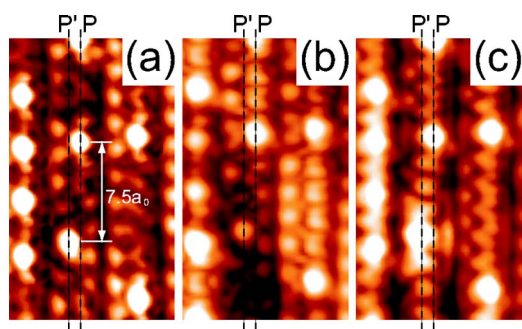
FIG. 7. (Color online) A Si adatom defect at biases (a) −0.4, (b) +0.4, and (c) +0.85. P and P' indicates the positions of normal Si adatoms and defective adatoms located on an alternative site, respectively.

Si adatom adsorption strongly influences adjacent states on β_1, i.e. Si atoms contributing to state D. As mentioned above, a dot subunit on a 5×4 unit or a short 5×2 chain (1- or $2-5\times2$-unit length) is imaged at an empty state lower in energy compared to those in a long 5×2 chain (over $2-5\times2$-unit length). Figure 6 shows normalized (dI/dV) spectra obtained inside and just outside a 5×4 Si adatom chain. It reveals that state D has a higher intensity and smaller width inside the chain than outside the chain. It is likely that state D inside the chain, confined by Si adatoms, may become moleculelike, whereas state D outside the chain, unhampered by Si adatoms, is spatially delocalized and becomes more dispersive, resulting in a broader and weaker state, as well as a lower binding energy.

V. ADATOM DEFECTS

Figure 7 shows a rarely observed Si adatom defect whose center is marked by line P'. This defect is intriguing in that it is a mirror image of a normal local unit cell with a Si adatom. As indicated in Fig. 7(a), two adatoms are separated by 2.93 nm $\sim 7.5a_0$ in the $[1\bar{1}0]$ direction, and spacing between P and P' in $[\bar{1}\bar{1}2]$ is a_0. This means that the relationship between these two are strikingly similar to that between Si adatoms across the dimer row in Si(111)-7×7, where one is located in the faulted half, and the other in the unfaulted half. This configuration can be obtained if the substrate with a normal Si adatom is rotated by 180 deg, and shifted by a_0 in the $[1\bar{1}0]$ direction, while leaving the dark row intact. The operation would place round units at the opposite side, and the substrate surrounding the Si adatom defect in a faulted half-configuration.

VI. MODELS FOR Si(111)-5×2-Au

Figure 8 shows two structure models proposed earlier: (a) was proposed by Marks and Plass (MP) based on a high-resolution electron microscopy and transmission electron diffraction study,[6] and (b) was suggested by Hasegawa, Hosaka, and Hosoki (HHH) from their STM images.[15] Both models include two rows of dimerized Au atoms located over Si missing rows, but the separations between two rows are dif-
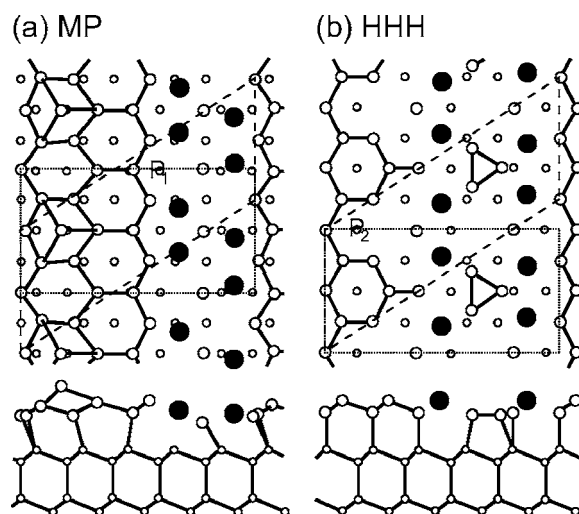
FIG. 8. Structure models for Si(111)-5×2-Au proposed by (a) Marks and Plass (MP) and (b) Hasegawa, Hosaka, and Hosoki (HHH). Empty circles represent Si atoms and filled circles represent Au atoms. Conventional (dashed lines) and STM-based rectangular (dotted lines) unit cells are added to guide the eye. Note that the direction of round and U units are reversed between MP and HHH models.

ferent. For the round units in STM images, MP model proposed a $2a_0$ periodic arrangement of Si adatoms, but the HHH model suggested Si trimers between two rows of Au. It should be noted that Si adatoms in MP model do not represent bright protrusions, but round units. The adsorption sites suggested by MP and HHH models for bright protrusions are P_1 and P_2, respectively. As a consequence, round and U units in the HHH model are reversed in comparison to those in the MP model. The direction of round and U units in the HHH model is in fact inconsistent with STM images and a surface orientation of a substrate.

Recently, Kang *et al.* theoretically examined the MP and HHH models for the Si(111)-5×2-Au surface without Si adatoms using density-functional theory calculations.[27] In their total-energy calculations, both models are found to be energetically sound: They are all locally stable and have almost identical adsorption energies. Both models, however, failed to reproduce key features of angle-resolved photoemission spectroscopy (ARPES) and STM results, indicating that a better model is needed.

More recently, based on works by Kang *et al.*, Erwin has proposed an improved model that is lower in the total energy than the other models, and that gives better agreements with photoemission data.[22] His model is shown in Fig. 9. Its unit cell is characterized by a double honeycomb chain, and a row of Si atoms half-removed. The removal of every other Si atoms located between α and β_1 in Fig. 9(a) not only makes sure the periodicity doubled to 5×2, but also keeps unsaturated Si dangling bonds in α rows. Here the dangling bonds would correspond to round units mentioned earlier. In Erwin's model, Si adatoms are assigned to H_3 sites marked by a plus sign in Fig. 9(a), and they are off-symmetric with respect to two round units, or two dangling bonds in row α. The stabilization of 5×4 comes from Si adatoms that supply
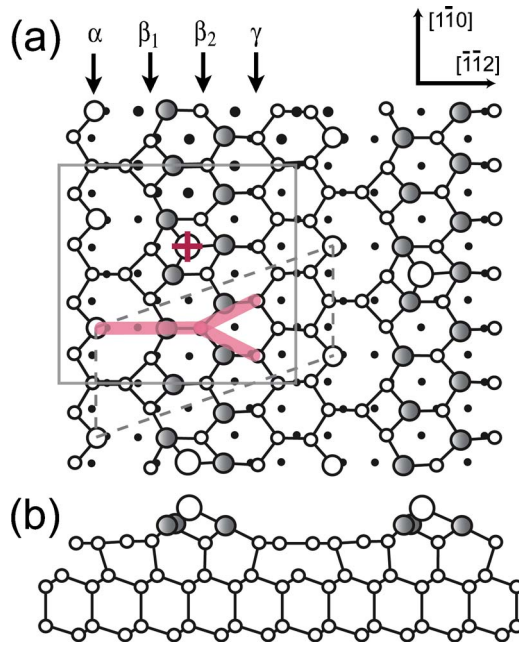
FIG. 9. (Color online) Erwin's model for Si(111)-5×2-Au. Black shaded circles represent Au atoms, and empty circles and dots represents the first and the second bilayer Si atoms, respectively, with the largest empty circles denoting Si adatoms. A conventional 5×2 unit cell and a STM-based 5×4 local unit cell are depicted by dashed lines and solid lines, respectively.

electrons that dope the 5×2 parent structure and thus lower the surface energy. Gray square indicates a local 5×4 unit cell observed by STM, and another gray "Y" unit lying on its side marks the position of a "Y" unit assigned by Erwin.

For comparison, our STM images with corresponding markings are shown in Fig. 10. Although it was claimed that the model agrees with photoemission data very well, there are a few conspicuous discrepancies in Erwin's model worth mentioning when compared to our STM images of Si(111)-5×2-Au surface.

First, the positions of Si adatoms, which are the most prominent and persistent features at this surface, are experimentally found symmetric with respect to each pair of round units, clearly noticeable in Fig. 10. However, the Si adatoms in Erwin's models, indicated by a plus sign in Fig. 10(a), are located off-symmetric with respect to round units. Placing the plus sign together with a square box, as shown in Fig. 10, clearly demonstrates that the plus sign does not lie at the center of a Si adatom. Relocating the Si adatom to the adjacent T_4 site may improve agreements with STM images, although at the cost of a significantly higher energy.[22]

Secondly, Y features, which appear only in Si adatom-free segments and low empty bias, are not found in the correct positions. A "Y" feature is a combination of a "V" head unit and a tail that ends at a round unit. Theoretical "V" comes from Si sites in Au−Si honeycomb structures in the model, with Au sites appearing dark in the STM image simulations. A comparison of the "Y" features made in Fig. 10(a) shows that theoretical "V" portion of "Y" falls completely within a dark region, with experimental "V" lying outside. In other words, experimental "V" is significantly shifted towards the
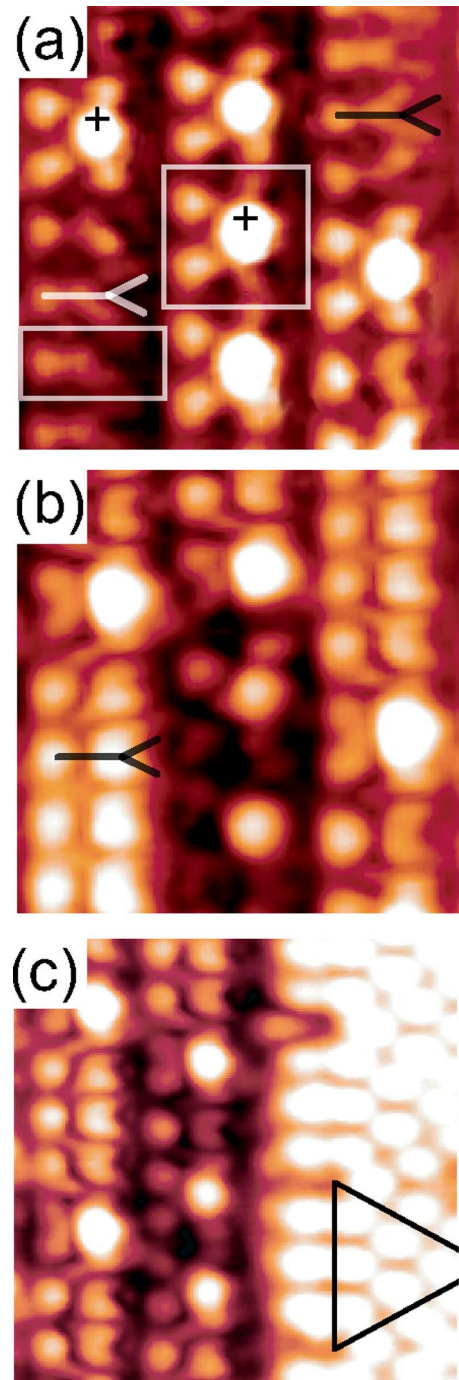
FIG. 10. (Color online) STM images of (a) filled state (−0.4 V) and (b) empty state (+0.4 V) of the same region on a Si(111)-5×2-Au surface. (c) shows a Si(111)-7×7 and Si(111)-5×2-Au coexistence region for the calibration purpose. A large square and a rectangle denote local 5×4 and 5×2 unit cells, while large circles within the rectangle denote Si adatom and Si atoms with dangling bonds, with a plus sign marking the position of a Si adatom. Small dots and medium-sized, shaded circles represent the second layer Si atoms and Au atoms, respectively. See the text for the discussion of "Y."

round unit, compared to the theoretical counterpart. In addition, if Si adatoms are located off-symmetric, as mentioned above, then a "Y" feature may be found in between $4a_0$

spaced Si adatoms, as drawn in Fig. 9(a). Round units are strongly affected by Si adatoms within the local unit cell, as observed in Fig. 5. If Si adatoms are located off-symmetric as in Erwin's model, then the round unit farther of the two will be less affected, turning on the "Y" feature. However, this was never observed experimentally, and "Y" features were always found in $6a_0$ or more wide Si adatom-free segments.

Third, Erwin's model exhibits strong LDOS along row γ, where the outer Si atoms of Si HC chains bond to Au atoms and are assigned to the top part of "Y." Simulated STM images in fact makes "V" part of the "Y" feature look barrel-shaped as a single bright piece. In contrast, STM images show that the corresponding region appear low in topography, or close to lowest, as found in Figs. 10(a) and 10(b), serving rather as a natural boundary separating from the neighboring rows. This is commonly found from the filled state up to 1.0 eV above E_F, at which point a new feature emerges, as shown in Fig. 2(f).

Figure 10(c) is shown for the calibration purpose. It shows not only a Si(111)-5×2-Au surface, but also Si(111)-7×7, with an equitriangle denoting a half-unit cell of 7×7 reconstructed Si surface. A comparison of three figures in Fig. 10 clearly shows that the two-fold symmetry exists in a local 5×4 unit cell. In this regard, our data does not agree with work by O'Mahony et al.[10] that presented seemingly off-symmetric images. The origin of the discrepancy may be traced to either severe thermal drift during scanning, or overdrift correction due to an improper determination of the inter-row phase slippage in their images. On the Si(111)-5×2-Au surface, the phase slippage between the ad-jacent rows occurs frequently, and it is difficult to determine the amount properly without the coexisting reference structures such as the Si(111)-7×7 surface. In fact, when the phase slippage between rows by the amount of a_0 in the reverse direction was forced upon their images, an excellent agreement with ours was achieved. On the other hand, a work by Baski et al.[8] presents a excellent agreement with our STM data.

Therefore, we find that Erwin's model does not give satisfactory agreements with our STM images of Si(111)-5 ×2-Au, and the true understanding of the surface structure is still lacking.

VII. CONCLUSIONS

In summary, we have performed an investigation of geometric and electronic structures of Si(111)-5×2-Au in detail using high-resolution STM and STS at low temperature. Our results revealed a topographical transition in STM images depending on bias voltages. A new atomic feature, V unit, and a local distribution of electronic states are observed by STM, STS, and CITS. The influences of state D and a Si adatom are found to be critical on both the geometric and electronic structure. In addition, our STM images of Si(111)-5×2-Au is found to be disagreed with the recently proposed structure models.

ACKNOWLEDGMENTS

*Electronic address: lyo@yonsei.ac.kr

[1] P. Segovia, P. Purdie, M. Hengsberger, and Y. Baer, Nature **402**, 504 (1999).

[2] H. E. Bishop and J. C. Riviere, Br. J. Appl. Phys. **2**, 1635 (1969).

[3] H. Lipson and K. E. Singer, J. Phys. C **7**, 12 (1974).

[4] Y. Yabuuchi, F. Shoji, K. Oura, and T. Hanawa, Surf. Sci. Lett. **131**, L412 (1983).

[5] S. M. Durbin, L. E. Berman, B. W. Batterman, and J. M. Blakely, Phys. Rev. B **33**, 4402 (1986).

[6] L. D. Marks and R. Plass, Phys. Rev. Lett. **75**, 2172 (1995).

[7] T. Hasegawa, K. Takata, S. Hosaka, and S. Hosoki, J. Vac. Sci. Technol. A **8**, 241 (1990).

[8] A. A. Baski, J. Nogami, and C. F. Quate, Phys. Rev. B **41**, 10247 (1990).

[9] J. D. O'Mahony, C. H. Patterson, J. F. McGlip, and F. M. Leibsle, Surf. Sci. Lett. **277**, L57 (1992).

[10] J. D. O'Mahony, J. F. McGilp, C. F. J. Flipse, P. Weightman, and F. M. Leibsle, Phys. Rev. B **49**, 2527 (1994).

[11] Y. Tanishiro and K. Takayanagi, Ultramicroscopy **31**, 20 (1989).

[12] T. Hasegawa, K. Takata, S. Hosaka, and S. Hosoki, J. Vac. Sci. Technol. B **9**, 758 (1991).

[13] T. Hasegawa, S. Hosaka, and S. Hosoki, Jpn. J. Appl. Phys., Part 2 **31**, L1492 (1992).

[14] T. Hasegawa, S. Hosoki, and K. Yagi, Surf. Sci. **355**, L295 (1996).

[15] T. Hasegawa, S. Hosaka, and S. Hosoki, Surf. Sci. **357**, 858 (1996).

[16] I. R. Collins, J. T. Moran, P. T. Andrews, R. Cosso, J. D. O'Mahony, J. F. McGlip, and G. Margaritondo, Surf. Sci. **325**, 45 (1995).

[17] I. G. Hill and A. B. McLean, Phys. Rev. B **55**, 15664 (1997).

[18] R. Losio, K. N. Altmann, and F. J. Himpsel, Phys. Rev. Lett. **85**, 808 (2000).

[19] K. N. Altmann, J. N. Crain, A. Kirakosian, J.-L. Lin, D. Y. Petro-vykh, F. J. Himpsel, and R. Losio, Phys. Rev. B **64**, 035406 (2001).

[20] J. R. Power, P. Weightman, and J. D. O'Mahony, Phys. Rev. B **56**, 3587 (1997).

[21] E. Bauer, Surf. Sci. Lett. **250**, L379 (1991).

[22] S. C. Erwin, Phys. Rev. Lett. **91**, 206101 (2003).

[23] T. Hasegawa and S. Hosoki, Phys. Rev. B **54**, 10300 (1996).

[24] Y. Yagi, K. Kakitani, and A. Yoshimori, Surf. Sci. **356**, 47 (1996).

[25] A. Kirakosian, J. N. Crain, J.-L. Lin, J. L. McChesney, D. Y. Petrovykh, F. J. Himpsel, and R. Bennewitz, Surf. Sci. **532–535**, 928 (2003).

[26] R. Bennewitz, J. N. Crain, A. Kirakosian, J.-L. Lin, J. L. Mc-Chensney, D. Y. Petrovykh, and F. J. Himpsel, Nanotechnology

13, 499 (2002).

[27] M.-H. Kang and J. Y. Lee, Surf. Sci. **531**, 1 (2003).

[28] H. S. Yoon, M.-A. Ryu, K.-H. Han, and I.-W. Lyo, Surf. Sci. **547**, 210 (2003).

[29] A. Kirakosian, R. Bennewitz, F. J. Himpsel, and L. W. Bruch, Phys. Rev. B **67**, 205412 (2003).

[30] H. S. Yoon, S. J. Park, J. E. Lee, C. N. Whang, and I.-W. Lyo, Phys. Rev. Lett. **92**, 096801 (2004).

[31] R. J. Hamers, R. M. Tromp, and J. E. Demuth, Phys. Rev. Lett. **56**, 1972 (1986).